



TECHNICAL NOTE

JFET Structural Analysis Report

		Name	Signature
Prepared by		Ruben Edeson	
		Iain Gilmour	
Approved by		J. Delderfield	



DISTRIBUTION

Name	Iss/Rev 1 Date 15/1/03	Iss/Rev 1.1 Date 23/1/03	Iss/Rev Date	Iss/Rev Date	Iss/Rev Date	Iss/Rev Date
Brockley-Blatt	x	x				
Bock	x	x				
Delderfield	x	x				

CHANGE RECORD

Date	Iss/Rev	Section	Comments
1/5/02	Draft 1		
8/5/02	Draft 2	6	Conclusions and recommendations added
8/8/02	Draft 3	1-6	Analysis re-run with CFRP mounting spacers
		Appendix 1	Bolt preload calculations appended.
15/1/03	Issue 1	Appendix 2	Preload test results added (I. Gilmour)
23/1/03	Issue 1.1	Various	Cosmetic changes to arrow positions in illustrations



<u>1</u>	<u>INTRODUCTION</u>	1
<u>2</u>	<u>APPLICABLE DOCUMENTS</u>	1
<u>3</u>	<u>FINITE ELEMENT MODEL DESCRIPTION</u>	1
<u>3.1</u>	<u>Assumptions</u>	2
<u>3.2</u>	<u>Material Properties</u>	3
<u>3.3</u>	<u>Model Mass Properties</u>	3
<u>4</u>	<u>MODAL ANALYSIS</u>	4
<u>4.1</u>	<u>Boundary Conditions and Loads</u>	4
<u>4.2</u>	<u>Results</u>	4
<u>5</u>	<u>STATIC LOADS ANALYSIS</u>	11
<u>5.1</u>	<u>Boundary Conditions</u>	11
<u>5.2</u>	<u>Applied Loads</u>	11
<u>5.3</u>	<u>Stress Results</u>	11
<u>5.4</u>	<u>Margins of Safety on Interface Screws</u>	12
<u>6</u>	<u>CONCLUSIONS</u>	16
<u>6.1</u>	<u>Modal</u>	16
<u>6.2</u>	<u>Static loads</u>	16
<u>6.3</u>	<u>Recommendations for Analysis</u>	16
<u>6.4</u>	<u>Recommendations for Testing</u>	16

1 INTRODUCTION

This report gives the results of analyses on the preliminary designs for both the 6-JFET and 2-JFET modules used on the SPIRE instrument. A modal analysis was performed on each model, followed by a quasi-static load analysis to simulate peak launch loads. This draft describes an analysis which includes thermal mounting spacers made from CFRP.

2 APPLICABLE DOCUMENTS

	Title	Number
AD1	Herschel/Planck IIDA	SCI-PT-IIDA-04624 Issue 3/0 01/07/02
AD2	Mechanical Properties of Corrosion Resistant Stainless Steel Fasteners - Part 1: Bolts, screws and studs.	BS EN ISO 3506-1: 1998
AD3	Selected Cryogenic Materials Data Notebook	CLRC Library C4031097
AD4	CYCOM 950-1/T300J Data Sheet	
AD5	Nonmetallic Materials and Composites at Low Temperatures (2) – Gunther Hartwig and David Evans.	CLRC Library C4005951
AD6	ISO Metric Screw Threads – Part 1: Principles and Basic Data	BS 3643-1: 1981

3 FINITE ELEMENT MODEL DESCRIPTION

An FEA model was produced each for the 2-JFET module and the 6-JFET module. The models were created in ANSYS 5.7.1 using solid data imported from Pro-Engineer CAD models. The models were defeatured in Pro-Engineer before importing into ANSYS.

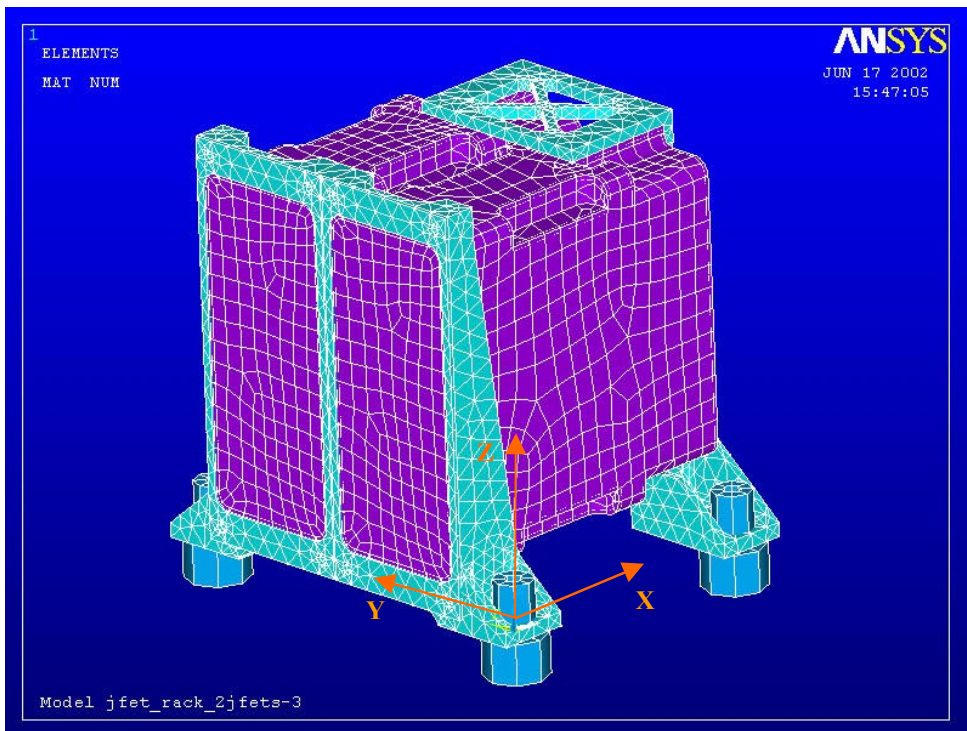


Figure 1 – The 2-JFET model

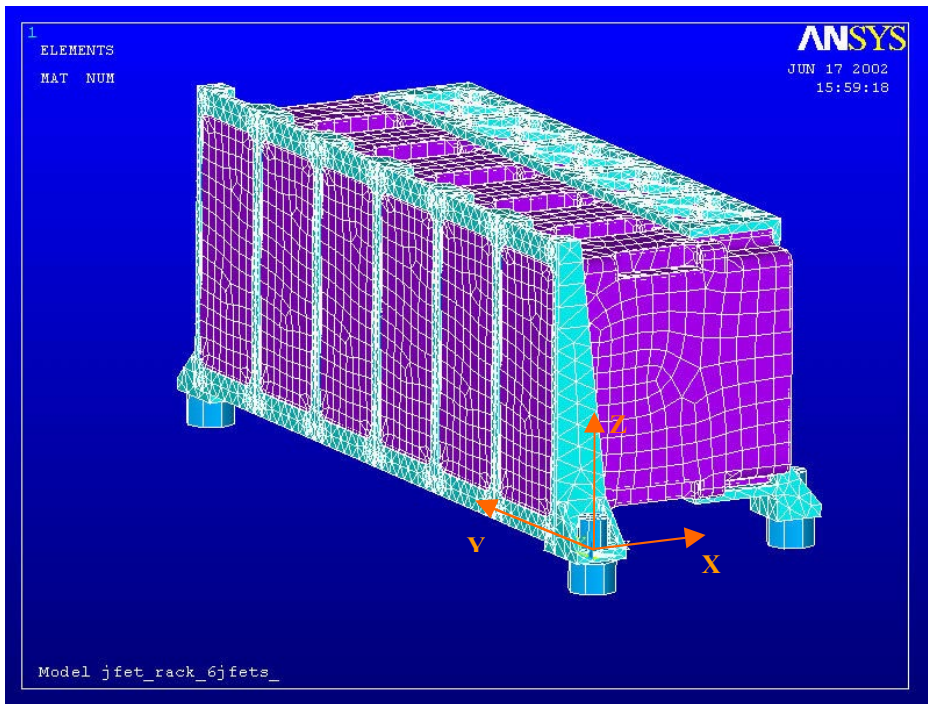


Figure 2 – The 3-JFET model

3.1 Assumptions

- All electrical connections and harnessing were ignored.
- Parts internal to the JFETs were ignored. The JFETs were modelled as 1mm thick Aluminium shells with densities adjusted to match the component mass of 305g.
- Attachment of the JFET flanges to the front support structure was made at four points using beam elements to model the screws.
- A node was used at the center of each mounting hole. It was attached to the mounting foot via stiff massless beam elements, and connected to a restrained node via a beam element representing the CFRP spacer. The restrained node was assumed to be on a rigid, stress free interface.

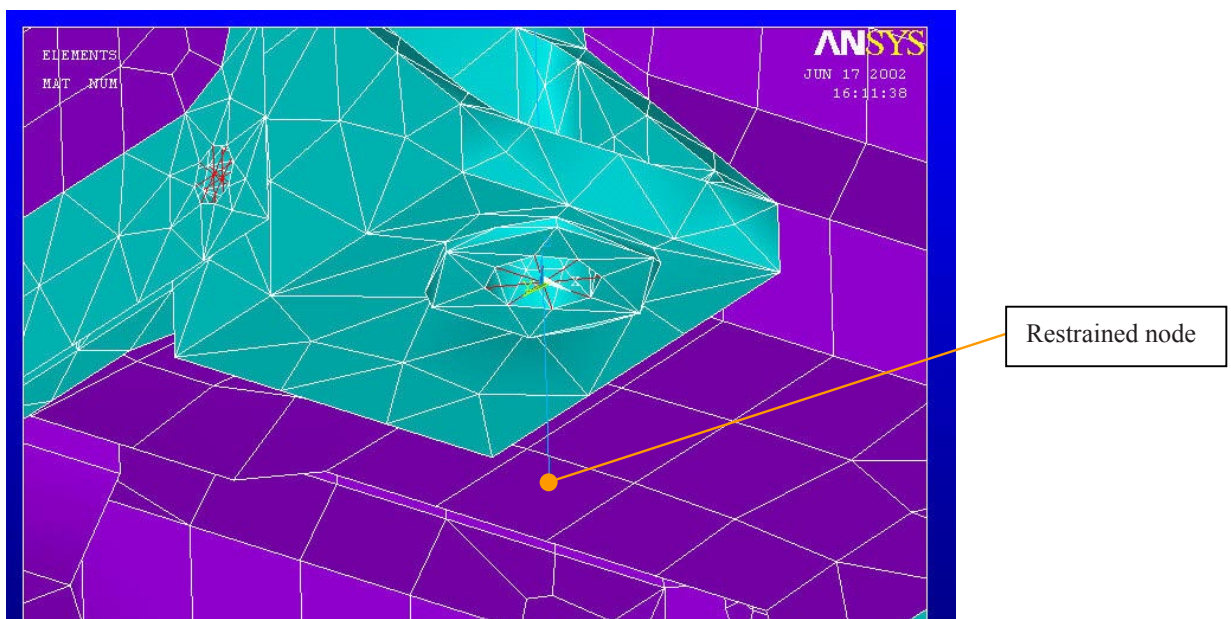


Figure 3 – Mounting foot node

- Thermal spacer dimensions were modelled as follows:

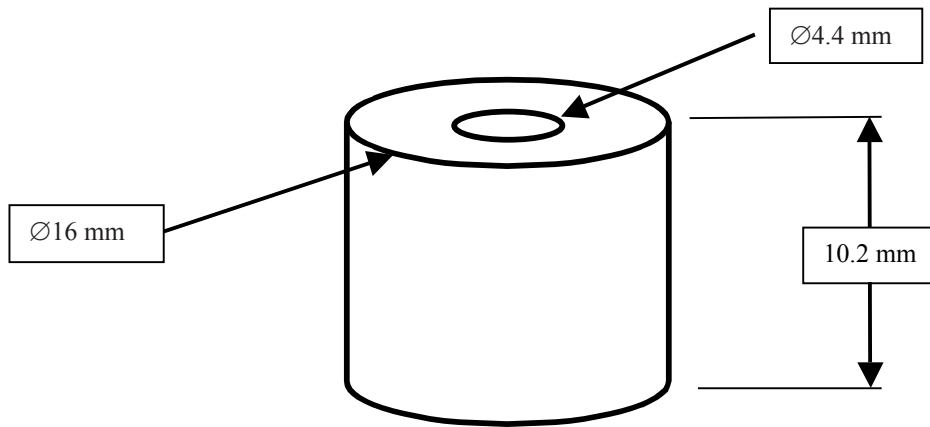


Figure 4 – Spacer Dimensions.

3.2 Material Properties

Material	Component(s)	Young's Modulus (GPa)	Density (Kg/m ³)	Poisson's Ratio
Aluminium Alloy	Panels	69	2720	0.30
Stainless Steel	Fastener links	204	-	0.30
JFETs	JFET Walls	69	11197	0.30
CFRP X dirn.	Mounting Spacers	8.8	1580	0.1 (XZ)
CFRP Y dirn.	Mounting Spacers	8.8	1580	0.1 (YZ)
CFRP Z dirn.	Mounting Spacers	112	1580	0.3 (XY)

- The first three materials exhibit isotropic behaviour.
- CFRP properties are estimated from AD4. The material is assumed to have uni-axial properties with high stiffness in the direction of bolt preload (the Z direction in Figures 1 and 2.)
- All properties are at room temperature.

3.3 Model Mass Properties

Mass properties for each model with respect to the mounting holes and reference frames indicated in Figures 1 and 2 are as follows (co-ordinates in mm):

3.3.1 2-JFET Model

Total Mass = 0.713 kg

COM (x, y, z) = (33.2, 48.2, 50.3)

3.3.2 6-JFET Model

Total Mass = 2.056 kg

COM (x, y, z) = (33.4, 129.3, 52.5)



4 MODAL ANALYSIS

4.1 Boundary Conditions and Loads

The restrained nodes were restricted only in translations. They were allowed rotations to give conservative results.

No loads were applied.

4.2 Results

4.2.1 2-JFET Model

The first 30 modes were taken out and tabulated below. Modes with effective masses above 10% of the rigid body mass are highlighted.

Mode	Frequency	EMM	EMM	EMM	Description
		X	Y	Z	
1	255.7	0.636	0.000	0.000	Rocking in X Direction
2	497.6	0.000	0.471	0.000	Side panels of JFETs
3	540.5	0.002	0.000	0.000	
4	541.2	0.000	0.009	0.000	
5	602.3	0.000	0.000	0.000	
6	799.6	0.000	0.063	0.000	Side panels of JFETs and rocking in Y direction
7	821.4	0.000	0.017	0.000	Twisting about Z-axis
8	999.2	0.001	0.000	0.502	Bouncing up and down in Z-direction
9	1011.0	0.000	0.033	0.000	
10	1022.4	0.000	0.000	0.009	
11	1027.8	0.000	0.074	0.000	Rocking in Y-direction; buckling of front bracket supports
12	1101.7	0.000	0.000	0.001	
13	1147.9	0.000	0.004	0.000	
14	1180.3	0.002	0.000	0.092	Side panels of JFETs
15	1181.6	0.000	0.010	0.001	
16	1302.0	0.014	0.000	0.002	
17	1322.4	0.000	0.002	0.000	
18	1329.3	0.000	0.000	0.002	
19	1384.1	0.034	0.000	0.051	Buckling of front bracket supports
20	1428.8	0.000	0.003	0.000	
21	1487.6	0.000	0.000	0.000	
22	1487.7	0.000	0.000	0.000	
23	1621.6	0.000	0.000	0.000	
24	1726.7	0.002	0.000	0.001	



Mode	Frequency	EMM			Description
		X	Y	Z	
25	1750.3	0.000	0.000	0.000	
26	1821.3	0.001	0.000	0.001	
27	1825.1	0.000	0.000	0.000	
28	1837.5	0.001	0.000	0.000	
29	1869.9	0.000	0.000	0.000	
30	1900.3	0.000	0.000	0.000	
Sum:		0.693	0.687	0.661	

Plots of selected modeshapes are shown below.

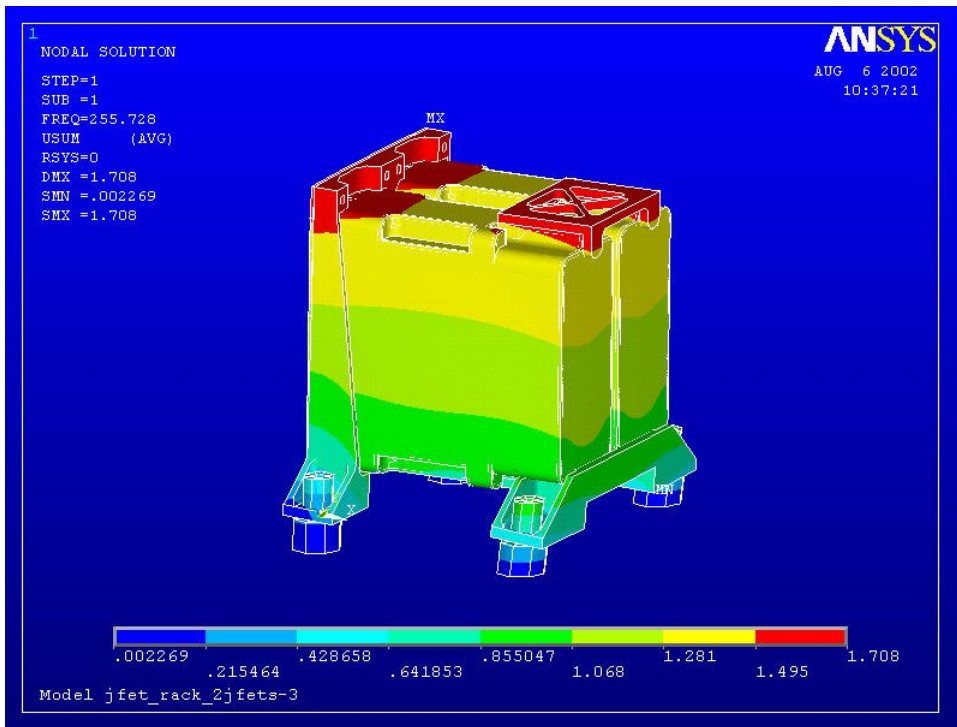


Figure 5 – Mode 1

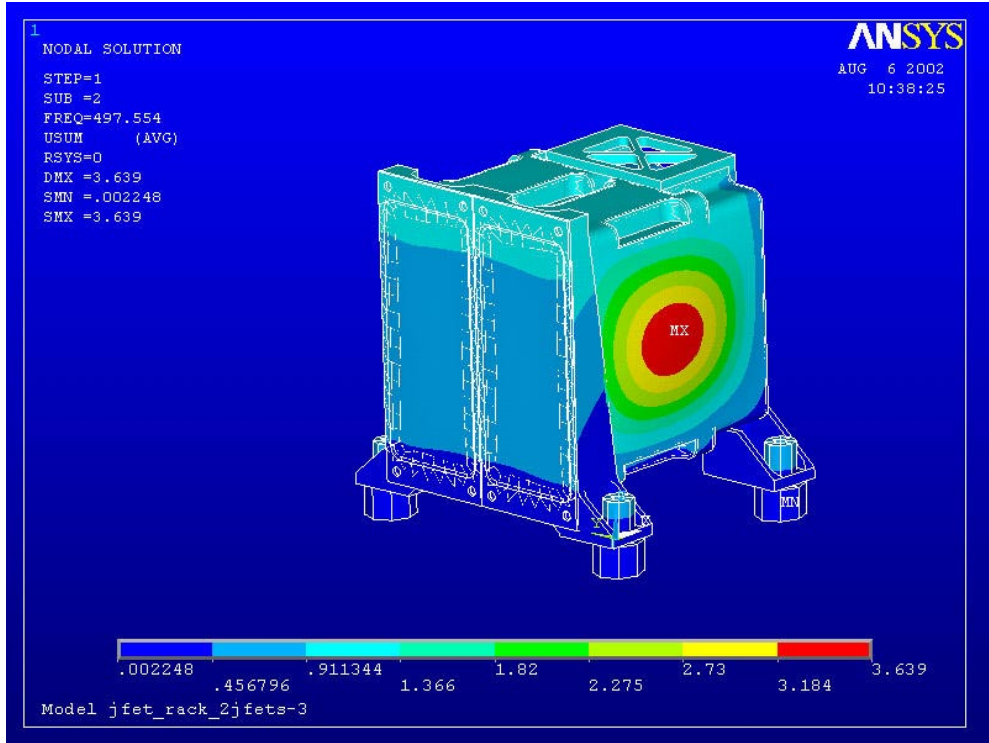


Figure 6 – Mode 2

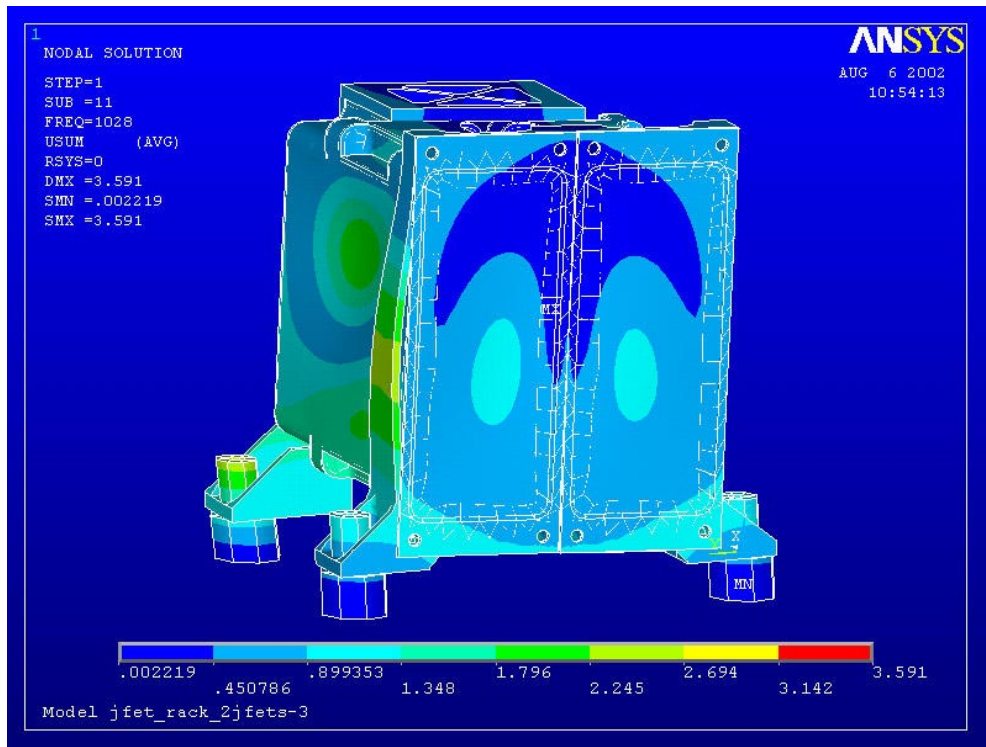


Figure 7 – Mode 11

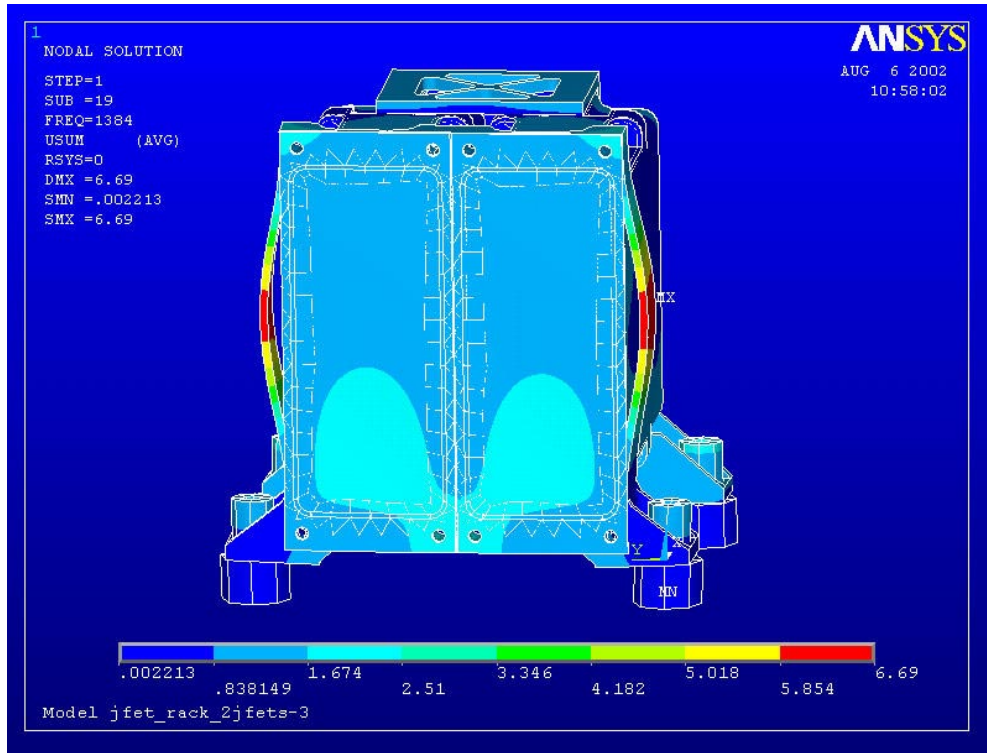


Figure 8 – Mode 19

4.2.2 6 JFET Case

The first 30 modes were taken out and tabulated below. Modes with effective masses above 10% of the rigid body mass are highlighted.

Mode	Frequency	EMM			Description
		X	Y	Z	
1	258.8	1.697	0.000	0.271	Translation of structure in X-direction
2	369.5	0.000	0.791	0.000	Twisting about Z-axis with translation in Y
3	427.7	0.000	1.064	0.000	Twisting about Z-axis with JFET panels structure acting as rigid body with deformations taken up in mounting feet.
4	540.7	0.000	0.000	0.005	JFET panel mode
5	543.3	0.000	0.002	0.000	
6	549.2	0.000	0.000	0.003	
7	550.5	0.000	0.000	0.000	
8	552.2	0.000	0.000	0.000	
9	553.7	0.000	0.000	0.000	
10	599.8	0.002	0.000	0.005	
11	604.8	0.000	0.000	0.000	
12	606.0	0.000	0.000	0.000	
13	606.5	0.000	0.000	0.000	



Mode	Frequency	EMM			Description
		X	Y	Z	
14	606.5	0.000	0.000	0.000	
15	698.0	0.253	0.000	0.639	Translation in the Z-direction
16	753.6	0.000	0.132	0.000	Translation in the Y-direction and JFET panels
17	970.3	0.002	0.000	0.001	
18	1009.3	0.000	0.000	0.000	
19	1015.4	0.000	0.000	0.002	
20	1016.2	0.000	0.000	0.000	
21	1017.1	0.000	0.000	0.000	
22	1027.8	0.001	0.000	0.000	
23	1064.1	0.000	0.002	0.000	
24	1068.5	0.002	0.000	0.006	
25	1094.3	0.000	0.000	0.000	
26	1104.2	0.000	0.000	0.001	
27	1104.3	0.000	0.000	0.006	
28	1105.8	0.000	0.000	0.002	
29	1105.8	0.000	0.000	0.000	
30	1120.0	0.004	0.000	0.045	
Sum:		1.963	1.992	0.985	

Plots of selected modeshapes are shown below:

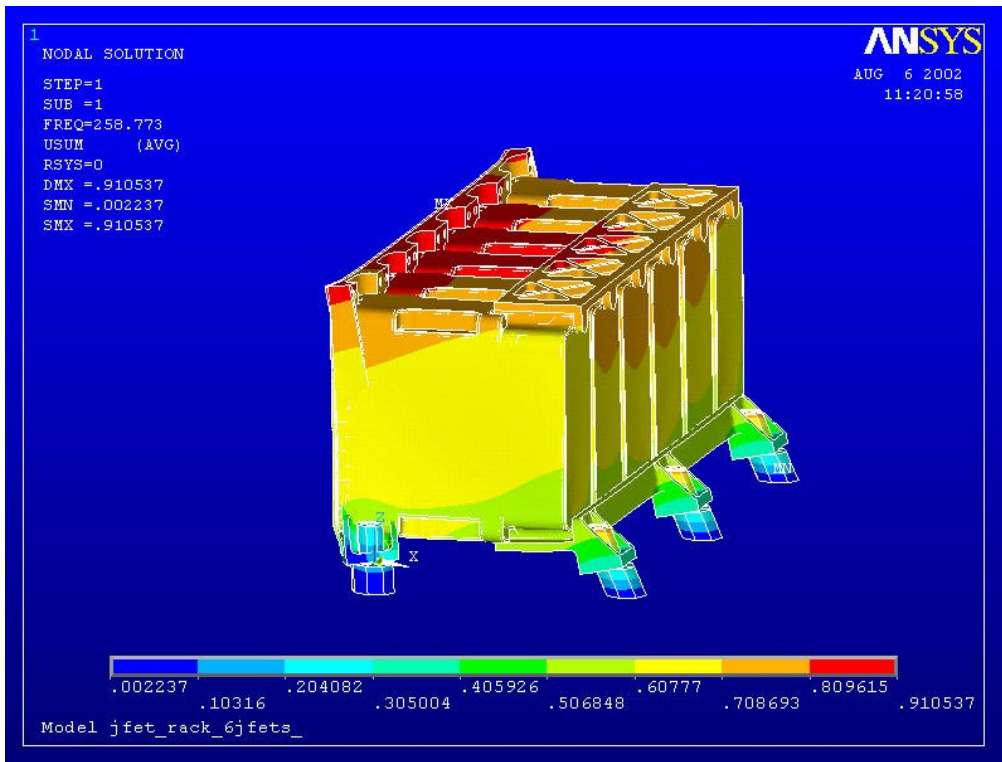


Figure 9 – Mode 1

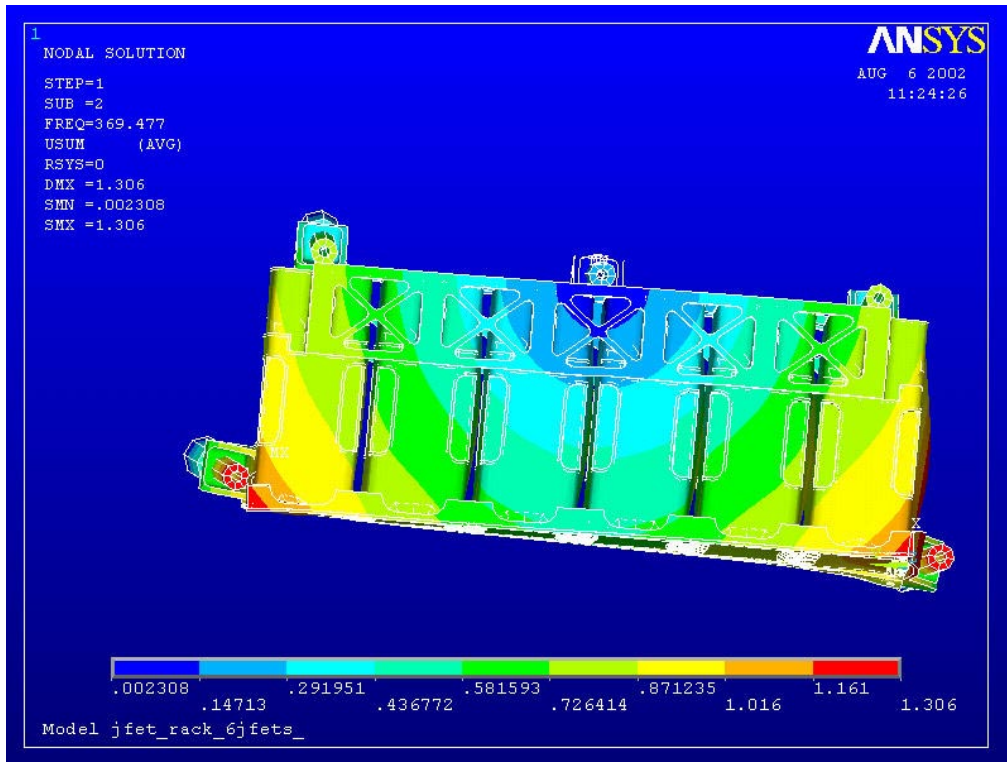


Figure 10 – Mode 2

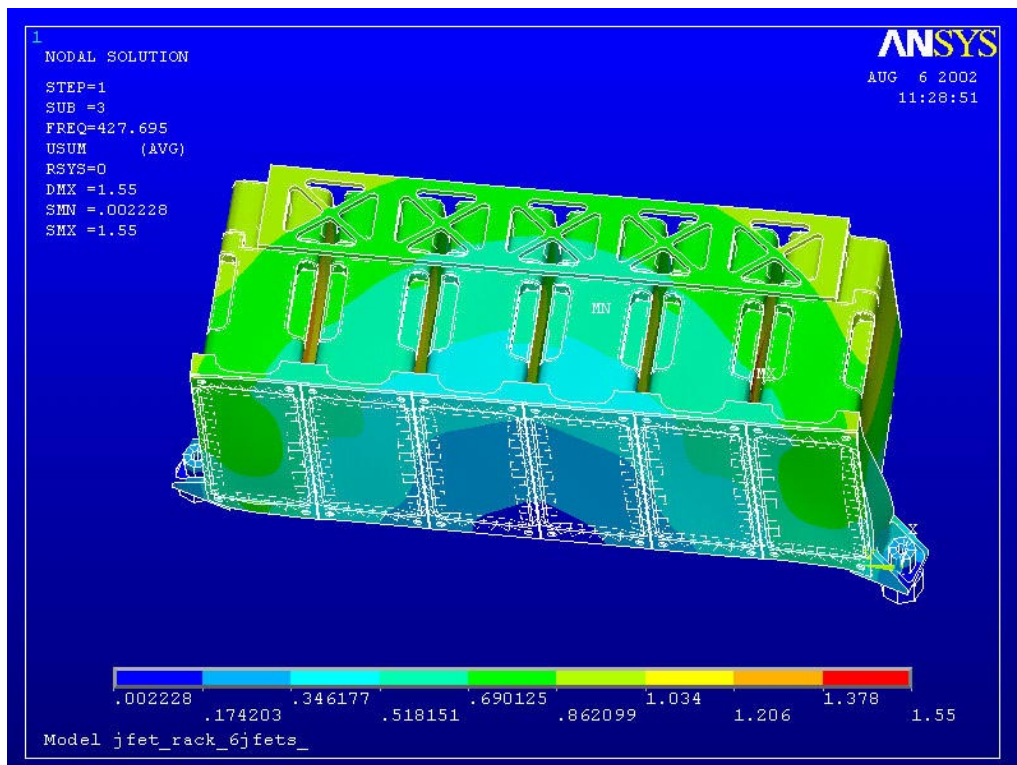


Figure 11 – Mode 3

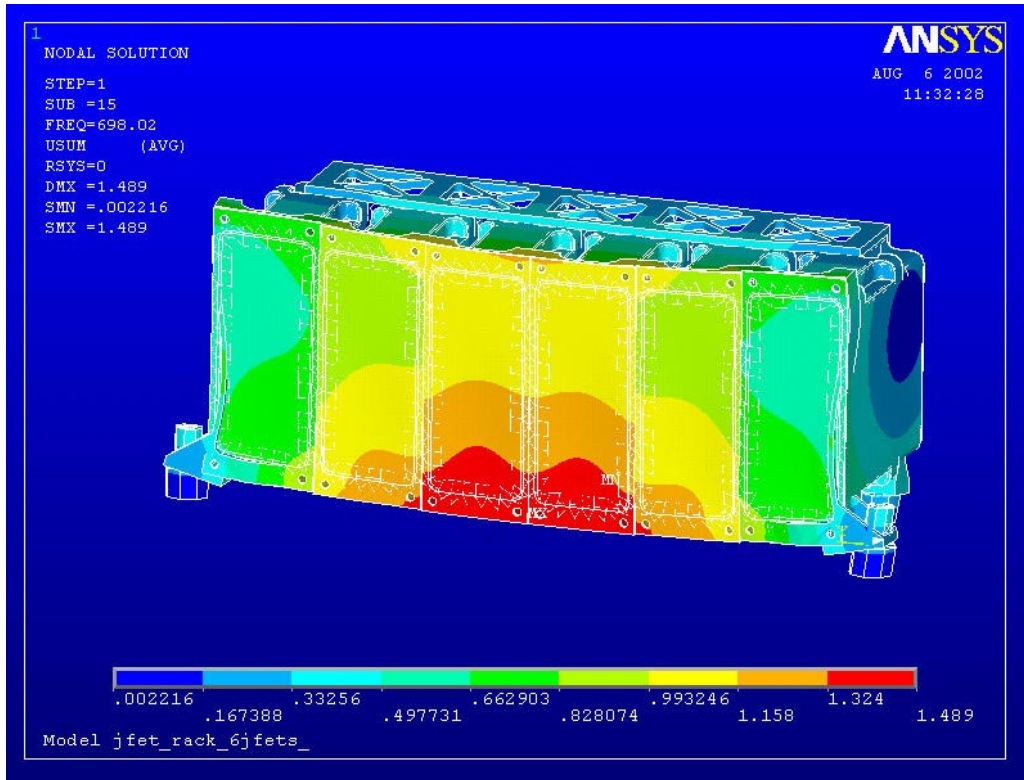


Figure 12 – Mode 15

5 STATIC LOADS ANALYSIS

5.1 Boundary Conditions

The nodes at the mounting feet were constrained in rotation as well as translation for this analysis.

5.2 Applied Loads

A load of 100g was applied in each orthogonal direction.

5.3 Stress Results

5.3.1 2 JFET Case

The maximum Von Mises equivalent stresses were:

	Maximum Stress (Mpa)	Location
100g in X Direction	250	Mounting foot screw hole
100g in Y Direction	166	JFET contact with rear bracket
100g in Z Direction	98	Mounting foot screw hole

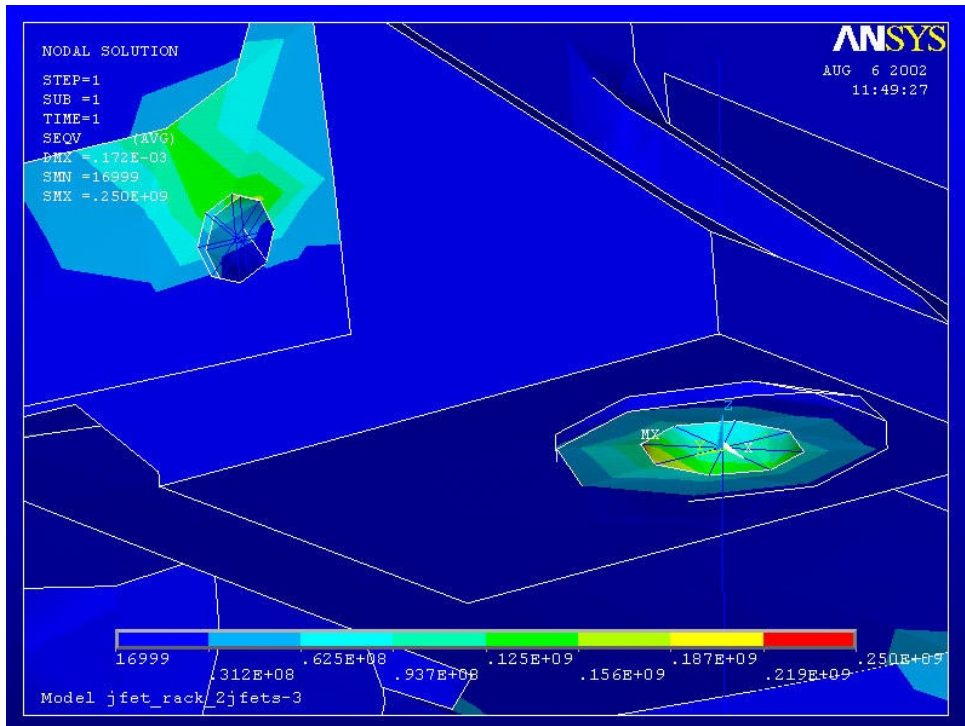


Figure 13 – Peak stress on mounting foot under X-direction loading. Note also high stress levels around the JFET mounting flange.



5.3.2 6 JFET Case

The maximum Von Mises equivalent stresses were:

	Maximum Stress (Mpa)	Location
100g in X Direction	324	Mounting foot screw hole
100g in Ydirection	166	Mounting foot screw hole
100g in Z Direction	297	Mounting foot screw hole

5.4 Margins of Safety on Interface Screws

5.4.1 MoS Equation

The margin of safety is given by (AD1):

$$\text{MoS (ultimate)} = (P_{\text{MAX}})/(P * K) - 1$$

Where:

P_{MAX} = Maximum allowable load according to failure criteria.

P = Actual applied load.

K = 2 (safety factor fromAD1)

5.4.2 Tensile Loading

The bolt preload at the launch temperature is given in Appendix 1.

$$P_{\text{PRELOAD}} = 4677\text{N}$$

The failure criterion in tension is assumed to be gapping, thus,

$$P_{\text{MAX}} = 4677\text{N}$$

5.4.3 Lateral Loading

For loading in the lateral direction, assume the failure criterion is sliding between the mounting spacers and their mounting interface.

From AD1 (Ch5, P29), assume the friction coefficient here to be:

$$\mu = 0.2$$

For each load case, the effective preload in the bolt resisting lateral motion through friction is this value minus the resulting axial load in the bolt.

$$P_{\text{BOLT}} = P_{\text{PRELOAD}} - Fz$$

Thus the maximum lateral Load is

$$P_{\text{MAX}} = 0.2*(4677 - Fz)$$

5.4.4 2 JFET Case

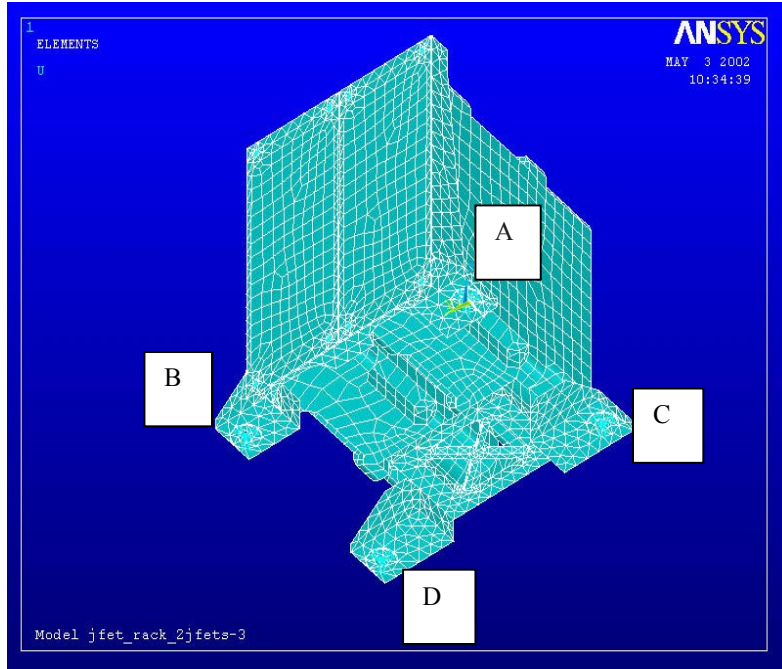


Figure 14 – Mounting hole designation

100g in X Direction								
Mounting Point	Node	FX (N)	FY (N)	FZ (N)	Tension (N)	Lateral (N)	MoS Tension	MoS Lateral
A	25333.0	118.6	55.3	210.0	210.0	130.9	10.136	2.414
B	25330.0	119.6	-55.7	212.7	212.7	131.9	9.995	2.384
C	25332.0	230.1	-314.9	-210.7	210.7	390.0	10.097	0.145
D	25331.0	229.7	315.4	-212.0	212.0	390.2	10.033	0.144
Total:		698.0	0.0	0.0				

100g in Y Direction								
Mounting Point		FX (N)	FY (N)	FZ (N)	Tension (N)	Lateral (N)	MoS Tension	MoS Lateral
A	25333.0	-43.2	159.8	232.0	232.0	165.5	9.078	1.685
B	25330.0	42.7	160.6	-231.9	231.9	166.2	9.086	1.675
C	25332.0	17.9	188.9	143.8	143.8	189.8	15.260	1.389



D	25331.0	-17.4	188.7	-144.0	144.0	189.5	15.238	1.393
Total:	0.0	698.0	0.0					

100g in Z Direction								
Mounting Point		FX (N)	FY (N)	FZ (N)	Tension (N)	Lateral (N)	MoS Tension	MoS Lateral
A	25333.0	-25.6	112.7	187.0	187.0	115.6	11.503	2.885
B	25330.0	-25.0	-112.9	187.0	187.0	115.7	11.505	2.882
C	25332.0	25.3	229.1	161.8	161.8	230.4	13.450	0.959
D	25331.0	25.3	-228.8	162.1	162.1	230.2	13.428	0.961
Total:	0.0	0.0	698.0					

5.4.5 6 JFET Case

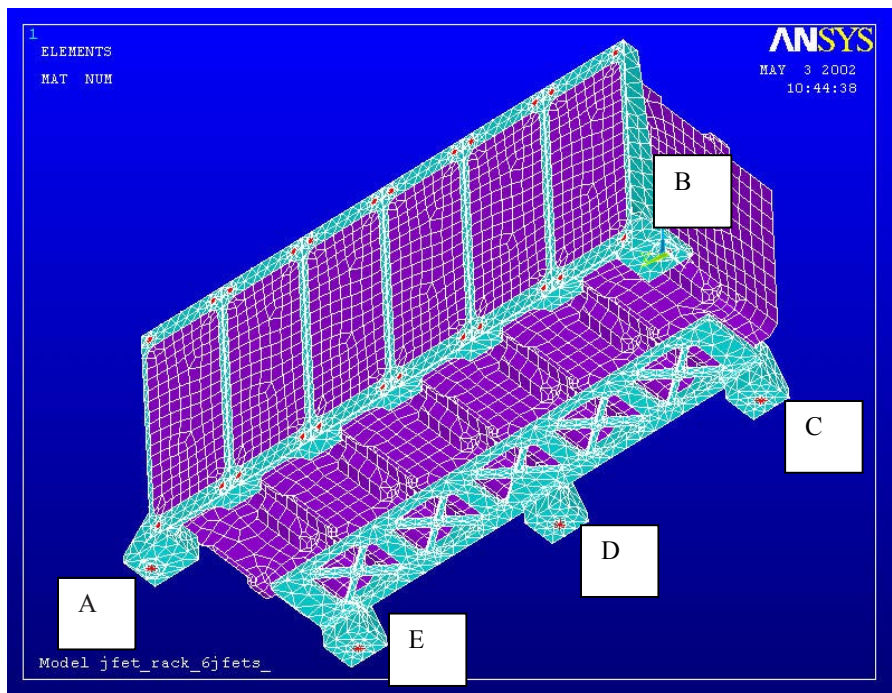


Figure 15 – Mounting hole designation

100g in X Direction								
Mounting Point	Node	FX (N)	FY (N)	FZ (N)	Tension (N)	Lateral (N)	MoS Tension	MoS Lateral
A	58472.0	23.3	-290.2	556.6	556.6	291.2	3.201	0.415
B	58473.0	22.0	290.3	555.9	555.9	291.2	3.207	0.415
C	58474.0	649.5	-61.9	-390.7	390.7	652.4	4.986	-0.343



D	58475.0	668.6	0.2	-330.6	330.6	668.6	6.073	-0.350
E	58471.0	650.1	61.6	-391.2	391.2	653.0	4.978	-0.344
Total:	2013.5	0.0	0.0					

100g in Y Direction								
Mounting Point		FX (N)	FY (N)	FZ (N)	Tension (N)	Lateral (N)	MoS Tension	MoS Lateral
A	58472.0	58.1	396.7	-225.9	225.9	401.0	9.354	0.110
B	58473.0	-58.6	394.4	225.6	225.6	398.7	9.366	0.116
C	58474.0	-82.4	353.9	229.0	229.0	363.3	9.213	0.224
D	58475.0	-0.2	514.7	0.4	0.4	514.7	5504.073	-0.091
E	58471.0	83.1	353.8	-229.1	229.1	363.4	9.206	0.224
Total:		0.0	2013.5	0.0				

100g in Z Direction								
Mounting Point		FX (N)	FY (N)	FZ (N)	Tension (N)	Lateral (N)	MoS Tension	MoS Lateral
A	58472.0	-37.2	-315.0	578.9	578.9	317.2	3.040	0.292
B	58473.0	-38.0	313.4	586.6	586.6	315.7	2.986	0.296
C	58474.0	102.0	77.3	159.9	159.9	128.0	13.621	2.529
D	58475.0	-129.7	1.6	519.2	519.2	129.7	3.504	2.206
E	58471.0	102.9	-77.3	159.8	159.8	128.6	13.633	2.511
Total:		0.0	0.0	2004.5				



6 CONCLUSIONS

6.1 Modal

Both models gave first natural frequencies above the 140 Hz minimum specified in AD1. This assumes material properties at room temperature. Launch is to occur at cryogenic temperatures though (around 10 K). AD3 shows that elastic moduli for both Stainless Steel and Aluminium alloys increases at these temperature. AD5 shows the same is true of CFRP. Hence this analysis is conservative.

In the 6-JFET case, a significant amount of effective mass was not taken out within the first 30 modes in the Z-direction.

6.2 Static loads

The assumed loading of 100g was greater than the design limit load given in AD1. At this loading, high stresses were found around the mounting feet of both models, though these were a result of the model restraint method.

Margins of safety for tension in all mounting screws were all above +1.

Margins of safety in the lateral directions were low and several were negative. The sensitivity of these results to static load acceleration levels, bolt preload, friction and applied safety factors was assessed:

- The highest acceleration possible (giving a worst case MoS of zero) is 66G.
- The bolt preload required to maintain a minimum MoS of zero (under a 100G load) is 7020N, which is not achievable even if the assumption of maximum preload during cooldown is relaxed.
- The minimum friction coefficient to give a worst case zero MoS (under a 100G load, with a 4266N preload) is 0.31.
- Relaxing the safety factor K from 2 to 1.29 gives a minimum zero MoS.

AD3 shown that the ultimate tensile strength of both materials increases at cryogenic temperatures, hence this analysis is also conservative.

6.3 Recommendations for Analysis

It is recommended that further analysis is carried out when the mounting design has been finalised, with the following changes:

- 6.3.1 More realistic modelling of the JFETS – many of the lower modes were associated with JFET panels. Giving them a realistic thickness and density would increase these frequencies.
- 6.3.2 Inclusion of accurate information on the material properties at the launch temperature.
- 6.3.3 Once the layup, resin, and fibre content of the CFRP spacers has been defined, further analysis should be performed to demonstrate that it will not fail in compression.

6.4 Recommendations for Testing

The application of bolt preload through differences in thermal contraction, as treated here, is completely analytical in nature. Tests should be performed to back up the assumptions made here. The application of preload using predefined bolt torques involves the use of safety factors based on statistical testing of bolts. A statistical approach should be taken in testing the temperature/preload relationship.

Because most of the contraction in the materials considered here occurs above 77K, such tests could be performed using liquid nitrogen. A torque wrench could be used to unload the bolt and assess the preload.

Tests should also be performed on the behaviour of the CFRP spacers at low temperatures. AD5 (PP245 – 258) found that internal delamination occurs on GFRP tubes over a certain thickness/diameter ratio.

Appendix 1 – Bolt Preloads.

The screws were assumed to be M4s to grade A2-80 with mechanical properties at room temperature.

The Ultimate Tensile Strength of the bolt material (from AD2) is:

$$\sigma_{UTS} = 800 \text{ Mpa}$$

The minimum Stress Area of an M4 Screw is:

$$A_{\sigma} = \pi(3.242)^2/4 \text{ mm}^2 \text{ (from AD6)}$$

$$= 8.255 \text{ mm}^2$$

Which gives a maximum permissible tensile load of:

$$P_{MAX} = 6604 \text{ N}$$

Under thermal contraction, assume the following configuration:

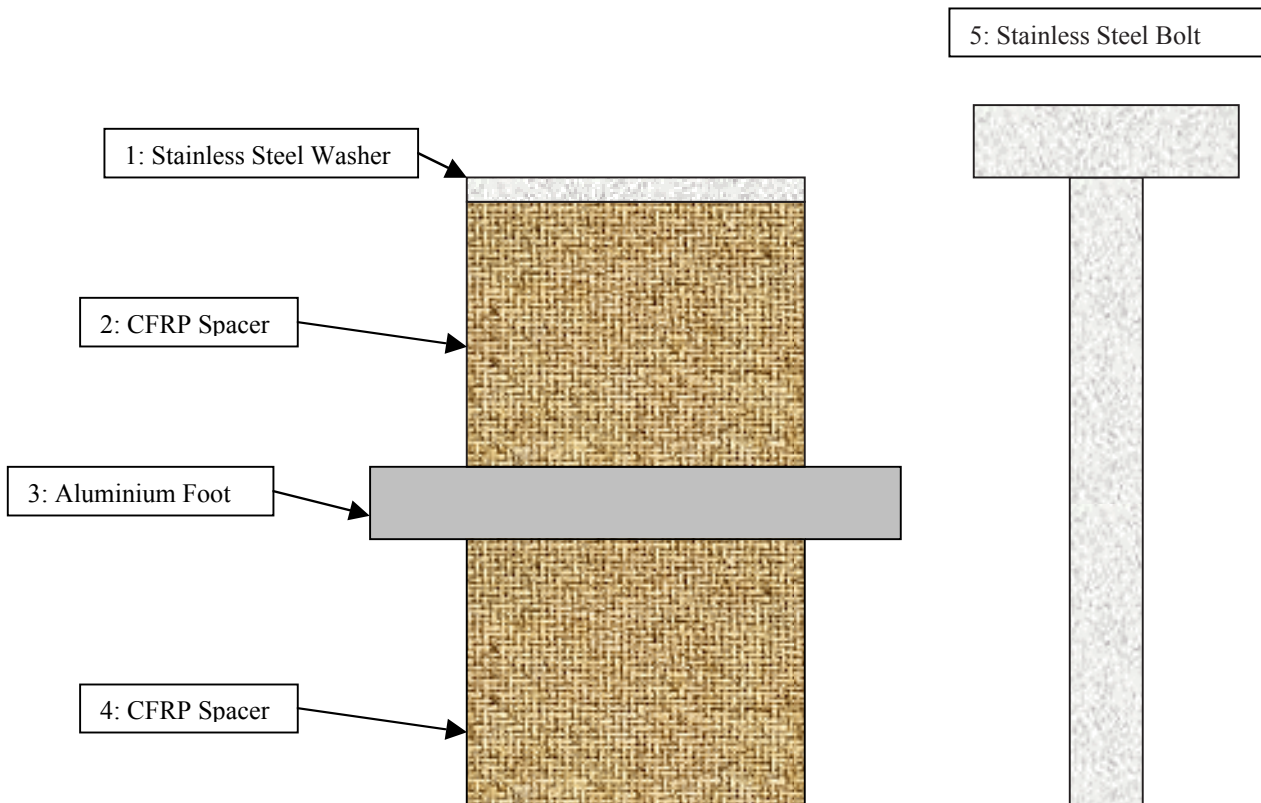


Figure 16 – Mounting Spacer Configuration.



Equating deformations due to bolt load with deformations due to thermal contraction:

$$\sum \delta_{elastic} = \sum \delta_{thermal}$$

Then :

$$P \sum_{i=1}^5 \left(\frac{L_i}{E_i A_i} \right) = \sum_{i=1}^5 L_i \left(\frac{\Delta L_{293-10}}{L_{293}} \right)$$

Where:

- P = tensile load in bolt (N)
- L_i = Length of element (mm)
- E_i = Young's Modulus of element at 10K (estimated from AD3, GPa)
- A_i = Cross sectional area of element (mm²)

$$\left(\frac{\Delta L_{293-10}}{L_{293}} \right) = \text{Total contraction over the range 293K - 10K}$$

The worst case for the bolt will be on cooldown where the bolt may have cooled significantly faster than the other elements of the joint, and therefore contracted to some extent before they have. A spreadsheet was created to solve the above equations and is summarised as follows.

Part	Material	L	Diameter	A	E	L/EA	dL/L(10K)	L[dL/L(10K)]	At 10K		On Cooldown	
									Load	Stress	Load	Stress
		mm	mm	mm ²	Gpa	m/N		m	N	Mpa	N	Mpa
1	St St	0.80	9.00	48.41	212.00	7.79E-11	2.96E-03	2.37E-06	-2510.41	51.86	-4437.26	91.66
2	CFRP Parr.	10.00	10.00	63.33	141.00	1.12E-09	-1.70E-04	-1.70E-06	-2510.41	39.64	-4437.26	70.06
3	Al	8.00		124.60	79.79	8.05E-10	4.15E-03	3.32E-05	-2510.41	20.15	-4437.26	35.61
4	CFRP Parr.	10.20	16.00	185.86	141.00	3.89E-10	-1.70E-04	-1.73E-06	-2510.41	13.51	-4437.26	23.87
5	St St	25.00	3.24	8.25	212.00	1.43E-08	2.96E-03	-7.40E-05	-2510.41	304.11	-4437.26	537.53
					Sum:	1.67E-08		-4.19E-05				

Note: Values in highlighted cells are estimated from AD5 (PP293-309). Values are negative because the material expands slightly on cooldown.

Thus on cooldown, the worst case load that will be applied to the bolt is 4437N. The maximum preload that can be put on the bolt before cooldown is 6604 – 4437 = 2167N.

If this maximum preload is applied to the bolt, then the preload in the joint at launch will be 2510 + 2167 = 4677N.

Appendix 1 – Bolt Preload Cryogenic Testing

Introduction

This investigation is concerned verifying the required room temperature torque to be applied to the Spire JFET fasteners in order to survive the launch vibration and the pre-launch cooldown.

The 2 JFET support assembly is shown in Figure 17. It should be noted that the previous analysis was concerned with a single case of an M4 bolt through a 25mm spacer. The current design calls for three cases, two bolts of different lengths and a stud with a nut.

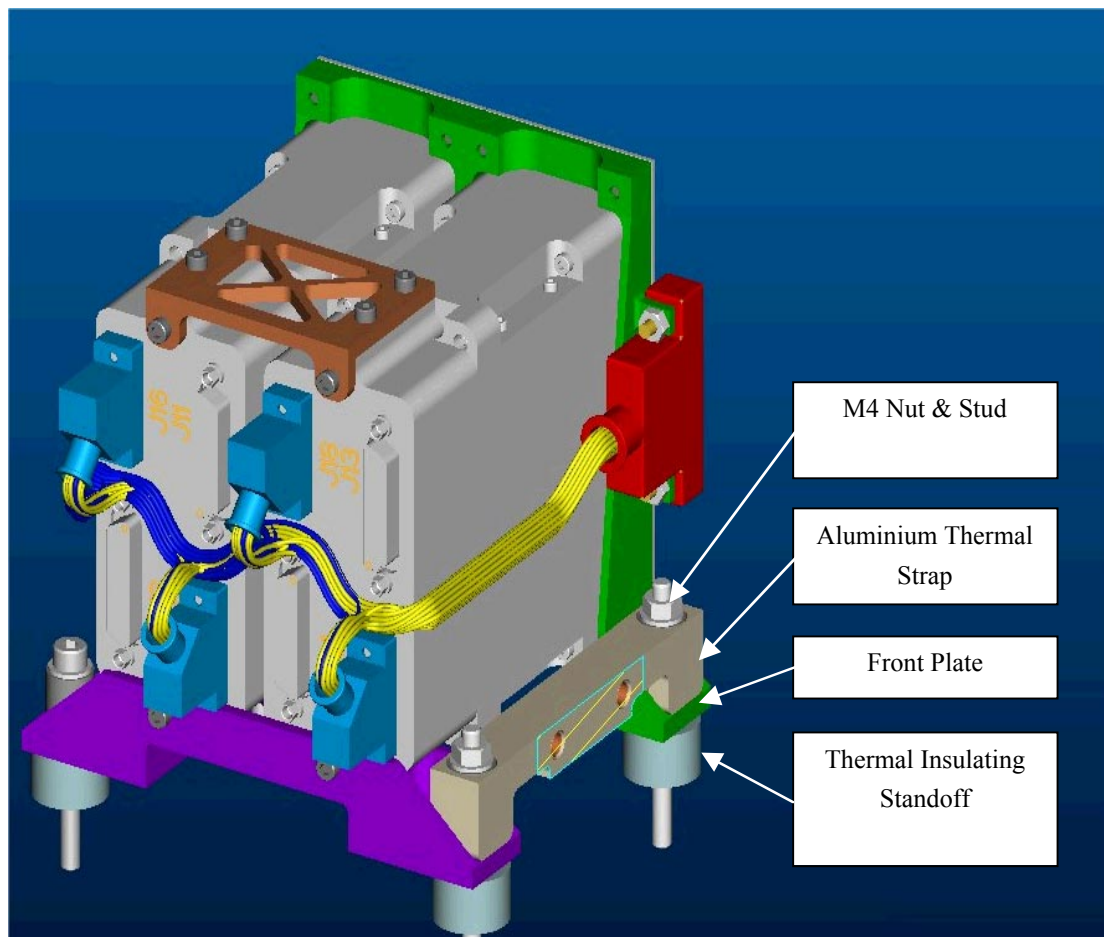


Figure 17

It is hoped to determine a room temperature torque to apply to the fasteners so that the sum of this preload and the preload induced by thermal contraction is sufficiently high without yielding the fastener or thermal standoffs.

This document describes the tests carried out in order to find a ‘safe’ preload and hence torque value to be applied at room temperature.

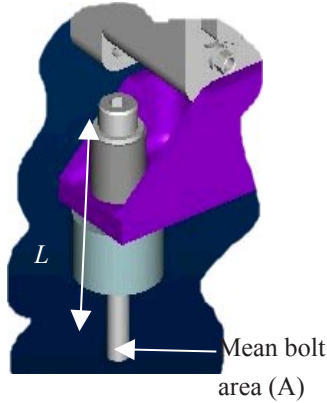
Test Setup

Young's Modulus states,

$$E = \frac{\sigma}{\epsilon} = \frac{(F / A)}{\Delta L / L}$$

Re-arranging this gives,

$$F = \frac{E \cdot A \cdot \Delta L}{L}$$



For Stainless Steel (AD3)

$E_{4K} = 212 \text{ GPa}$

$E_{300K} = 204 \text{ GPa}$

If the change in length of the fastener can be measured, the preload can be calculated. Figure 2 shows the test apparatus designed to find the change in length across the components.

The thermal isolating standoffs, thermal strap and foot beam dummies are stacked up around the fastener as represented in the flight model. However, the washer representation is noticeably different to a normal standard M4 washer. It was designed to be representative of a standard M4 washer in compression and to support a location for the extensometer. The other location for the extensometer screws into the base plate.

There are 3 different test set-ups to represent the flight model fasteners: 1 – “bolted with no thermal strap”, 2- “bolted with no thermal strap” (shown in figure 18), 3- “stud with a thermal strap” - fastened with a special M4 nut (KE-0104-386).

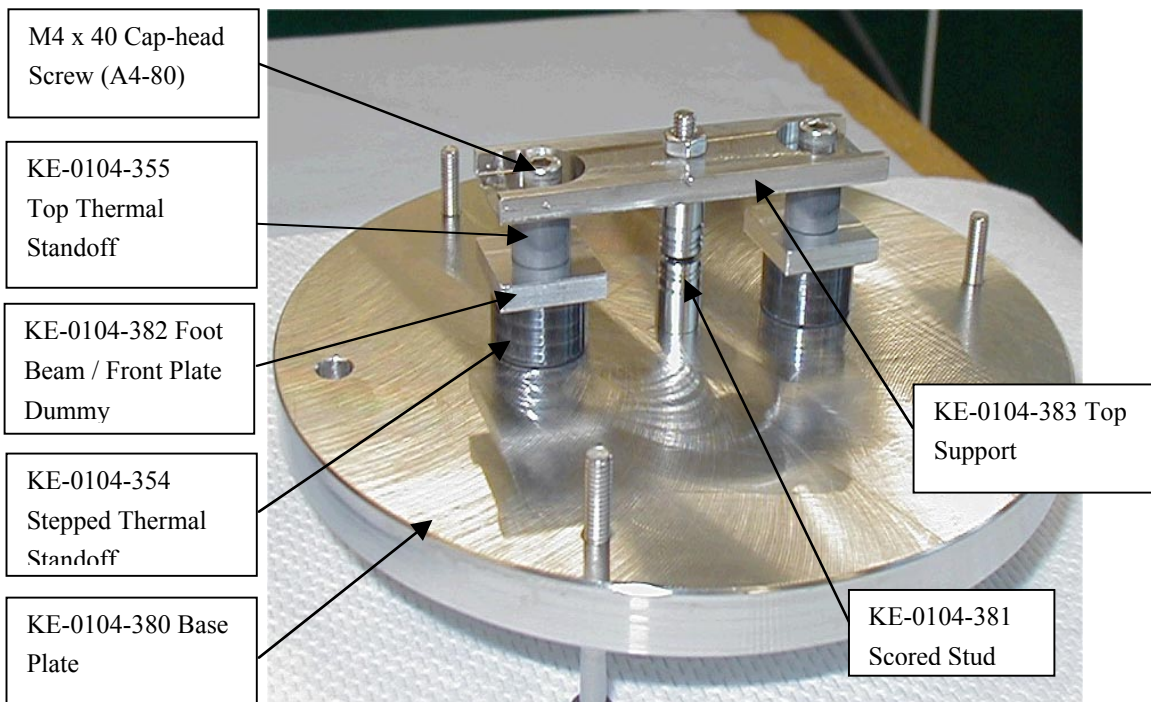


Figure 18

Testing

For each test it was necessary to find the natural unloaded change in length of the bolt or stud due to thermal contraction. The natural change in length was subsequently subtracted from a test with all the components stacked up with very small torque (0.06Nm was the smallest achievable) in order to find the preload induced in the fastener due to thermal contraction. The cooling was done by lowering into a dewar of liquid helium.

In AD 1 it was stated that the minimum preload required in the fasteners was 4.0kN. If the preload due to thermal contraction can be calculated as described above, the remaining preload to be applied is that due to the room temperature torque.

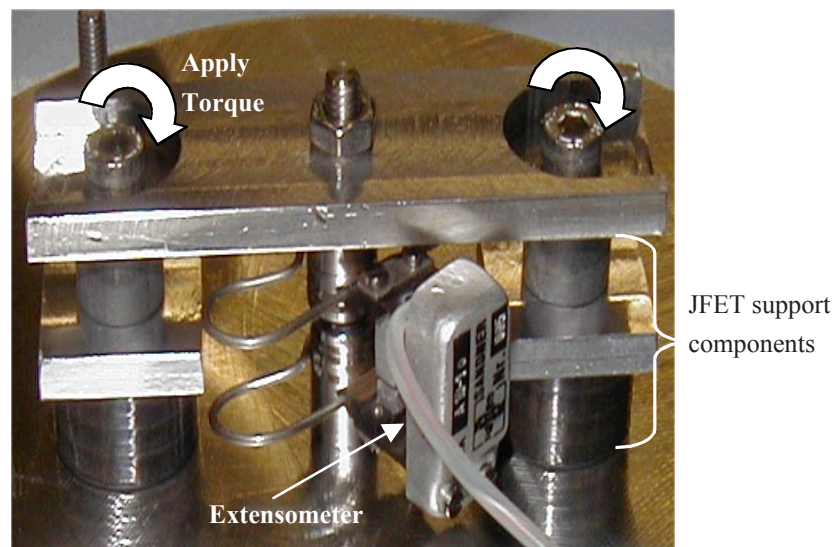
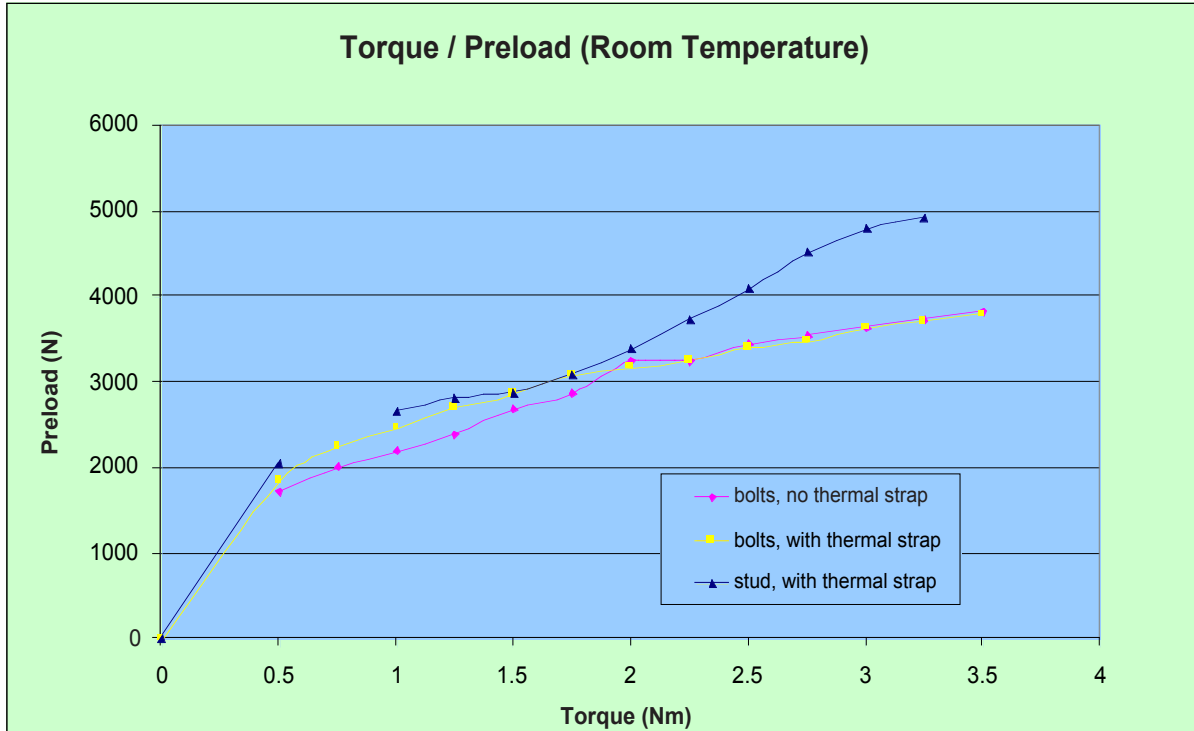


Figure 3

In order to find the preload at a given value, torque values ranging from 0 to 3.5Nm were applied to the fasteners and the change in length was measured (Figure 3). From these values a graph of room temperature preload against torque could be plotted. It should be noted that the stainless steel stud was coated with Tungsten Disulphide (applied by *WS2 Coatings Ltd.*) in order to reduce friction. A small amount of threading lubricant was used on thread engagements within test apparatus.

Results

Room temperature torque / preload relationships



Note: these curves were produced using a theoretical equivalent stiffness for the bolted members.

Preload due to thermal contraction in liquid helium (4K)

NB. Inconsistencies in the extensometer readings led to a large range of possible preloads in the fasteners. In order to increase confidence in the calculations, an error analysis was carried out which led to the suggested values.

Test Setup	Thermal Contraction over 10mm (um)	Contraction over fastener length (um)	Delta L loaded (um)	Thermal Preload (N)
1 = bolts, no thermal strap	18.6	46.5	34	931
2 = bolts, with thermal strap	18.6	53.9	27	1729
3 = studs, with thermal strap	18.6	60	32	1714

* It was noticed that the thermally induced preload (931N) in Test 1 was unexpectedly low as it should have been at least equal to those in tests 2 & 3 since there is less material to contract with the fastener.



Test 1 was repeated with a 3.5Nm torque on the bolts as a survival test and also to note any observations. The test was successful and it was calculated that the thermal preload should have been approximately equal to those in tests 2 & 3. The calculated value was 1723N which suggests that the contraction difference between each test was not noticeable within the capabilities of the test equipment.

The total error in these results, based on the spread of results over 5 identical test cases, is over 100%. The $\pm 12\mu\text{m}$ Root Sum of Squares error equates to about $\pm 800\text{N}$.

Suggested Fastener Torques

Since the 3.5Nm torque survival test was successful, it was decided to round the required torque up to the nearest kilonewton in order to be confident that enough preload is applied. Therefore, reading across from 3.0kN on the torque/preload graph suggests that 2.0Nm should be used in all cases. Adding the 1.7kN preload induced by thermal contraction gives a total preload of about 4.7kN.

If it is found at any time that 2.0Nm does not induce enough preload (i.e. the fastener becomes loose), the torque can be increased below 3.5Nm – above 3.5Nm there is no guarantee that the components will survive.

Test Setup	Required Preload (N)	Required Preload Prior to Cool-down (N)	Suggested Minimum Torques (Nm)
1 = bolts, no thermal strap	4200	2477	2
2 = bolts, with thermal strap	4200	2471	2
3 = studs, with thermal strap	4200	2486	2

These torques are based on a lubricated thread engagement with the test fixture. Any extra torque required to overcome friction (ie, from locking threads) should be added to cases 1 and 2.

Conclusion on Fastener Torques

The room temperature torque-preload characteristics of the three cases were measured using an assumed theoretical bolted member stiffness. The assessment of preload induced by thermal differential was problematic with large experimental errors from the test equipment as well as assumptions about material behaviour at low temperatures. Ideally a statistical approach would have been taken, with room temperature torque versus low temperature preload being assessed over a range of torques.

However, the survival test, which was carried out on ‘worst case’ test configuration for stress, was successful. The applied room temperature torque was 3.5Nm which, when taking into account the preload induced by cool-down, induced a higher preload than specified. Inspection of the thermal standoffs showed no noticeable defects and the extensometer reading returned to zero, thus indicating that no permanent deformation had occurred. It is suggested that survival tests are carried out on cases 2 and 3 with the recommended torques given here.